Cortactin Localization to Sites of Actin Assembly in Lamellipodia Requires Interactions with F-Actin and the Arp2/3 Complex

Scott A. Weed,* Andrei V. Karginov,* Dorothy A. Schafer,‡ Alissa M. Weaver,‡ Andrew W. Kinley,* John A. Cooper,‡ and J. Thomas Parsons*

*Department of Microbiology and Cancer Center, University of Virginia Health Sciences Center, Charlottesville, Virginia 22908; and ‡Department of Cell Biology and Physiology, Washington University School of Medicine, St. Louis, Missouri 63110

Abstract. Cortactin is an actin-binding protein that is enriched within the lamellipodia of motile cells and in neuronal growth cones. Here, we report that cortactin is localized with the actin-related protein (Arp) 2/3 complex at sites of actin polymerization within the lamellipodia. Two distinct sequence motifs of cortactin contribute to its interaction with the cortical actin network: the fourth of six tandem repeats and the amino-terminal acidic region (NTA). Cortactin variants lacking either the fourth tandem repeat or the NTA failed to localize at the cell periphery. Tandem repeat four was necessary for cortactin to stably bind F-actin in vitro. The NTA region interacts directly with the Arp2/3 complex based on affinity chromatography, immunoprecipitation assays, and binding assays using purified components. Cortactin variants containing the NTA region were inefficient at promoting Arp2/3 actin nucleation activity. These data provide strong evidence that cortactin is specifically localized to sites of dynamic cortical actin assembly via simultaneous interaction with F-actin and the Arp2/3 complex. Cortactin interacts via its Src homology 3 (SH3) domain with ZO-1 and the SHANK family of postsynaptic density 95/dlg/ZO-1 homology (PDZ) domain–containing proteins, suggesting that cortactin contributes to the spatial organization of sites of actin polymerization coupled to selected cell surface transmembrane receptor complexes.

Key words: actin • cortactin • lamellipodia • Arp2/3 complex

Introduction

Dynamic regulation of the actin cytoskeleton plays a central role in a variety of cellular events, including adhesion, division, spreading, and motility (Mitchison and Cramer, 1996). Engagement or activation of cell surface growth factors and adhesion receptors influences the assembly and arrangement of F-actin networks (Zigmond, 1996; Schoenwaelder and Burridge, 1999). Transmission of extracellular signals to the actin cytoskeleton is governed by small GTPases of the Rho family, as well as by the activity of numerous actin-binding proteins (Ayscough, 1998; Hall, 1998).

The Rho family GTPases, Cdc42 and Rac, play a critical role in the formation and organization of cortical actin networks in mammalian cells. Treatment of cells with agents that increase GTP-bound Cdc42 stimulates filopodia formation (Kozma et al., 1995), whereas activation of Rac leads to membrane ruffle and lamellipodia formation (Ridley et al., 1992). Formation of cortical actin networks, resulting either from EGF stimulation (Chan et al., 1998) or activated Rac (Machesky and Hall, 1997), requires de novo formation of F-actin filaments, indicating that Cdc42 and Rac integrate signal pathways leading to actin polymerization. In addition, Rac activation is closely coupled to activation of Cdc42 (Nobes and Hall, 1995), allowing for the coincident and coordinated formation of filopodia and lamellipodia that are often concurrently observed at the leading edge in motile cells (Rinnerthaler et al., 1988). Actin polymerization at the leading edge provides the protrusive force required for the extension of lamellipodia observed during cell motility and spreading (Small et al., 1999).

Cortical actin polymerization initiated by Cdc42 and Rac requires the participation of members of the Wiskott-Aldrich Syndrome protein (WASp)[1] superfamily (Bi and

Address correspondence to J. Thomas Parsons, Department of Microbiology, Box 800734, University of Virginia Health Sciences Center, Charlottesville, VA 22908-0734. Tel.: (804) 924-5395. Fax: (804) 924-1071. E-mail: jtp@virginia.edu

S.A. Weed's present address is School of Dentistry, Department of Basic Sciences and Oral Research, Box C286, University of Colorado Health Sciences Center, 4200 East Ninth Avenue, Denver, CO 80262.

[1]*Abbreviations used in this paper:* Arp, actin-related protein; CMV, cytomegalovirus; CortBP-1, cortactin-binding protein 1; GFP, green fluorescent protein; GST, glutathione *S*-transferase; LC-MS, liquid chromatography mass spectrometry; NTA, amino-terminal acidic domain; PDZ, PSD95/dlg/ZO-1 homology; PSD, postsynaptic density; Scar, suppressor of cAr; SH, Src homology; SHANK, SH3 domain and ankyrin repeat protein; VCA, verpolin homology, cofilin, and acidic domain contained in the COOH-terminal fragment of N-WASp; WASp, Wiskott-Aldrich Syndrome protein.

Zigmond, 1999). Binding of activated Cdc42 to N-WASp induces filopodia (Miki et al., 1998a), whereas Rac-induced membrane ruffling utilizes the structurally related protein Scar1 (also known as WASp family verpolin-homologus protein [WAVE]) (Machesky and Insall, 1998; Miki et al., 1998b). All WASp/Scar family proteins contain a carboxyl-terminal motif rich in acidic residues, which is responsible for their activity (Higgs and Pollard, 1999) and mediates binding to the actin-related protein (Arp) 2/3 complex (Machesky and Gould, 1999). Arp2/3 complexes consist of the actin-related proteins Arp2 and Arp3 along with five other proteins designated p41-, p34-, p21-, p20-, and p16-Arc (Machesky and Gould, 1999) (also designated as ARPC1–5).

Arp2/3 complex binds to the sides of preexisting actin filaments and stimulates new filament formation to create branched actin networks, a process termed the "dendritic nucleation" model of cortical actin assembly (Mullins et al., 1998). As predicted by this model, the Arp2/3 complex is located at branch points of actin filament networks in lamellipodia, as seen by electron microscopy (Svitkina and Borisy, 1999), and is localized to sites of dynamic actin assembly and motility in living cells (Schafer et al., 1998). Arp2/3-induced actin nucleation and polymerization are greatly enhanced by the binding of WASp family acidic carboxyl-terminal domains to p21-Arc (Machesky and Insall, 1998), thus providing a molecular link for Cdc42 and Rac leading to cortical actin polymerization (Machesky et al., 1999; Rohatgi et al., 1999).

In addition to the Arp2/3 complex, several actin binding proteins are selectively recruited into cortical actin structures upon activation of Cdc42 or Rac (Kobayashi et al., 1998; Mishima and Nishida, 1999; Kessels et al., 2000), including the Src kinase substrate cortactin (Wu et al., 1991), an actin binding protein enriched within lamellipodia (Wu and Parsons, 1993). The localization of cortactin within membrane ruffles and lamellipodia is controlled by activation of Rac (Weed et al., 1998). Cortactin possess a multidomain structure consisting of an acidic domain at the amino terminus, followed by 6 and 1/2 tandemly repeated 37–amino acid segments, an α helical region, a proline-rich segment, and a Src homology (SH) 3 domain located at the carboxyl terminus (Wu et al., 1991). The direct binding to F-actin is mediated through sequences within the tandem repeat region (Wu and Parsons, 1993). The SH3 domain interacts with several postsynaptic density (PSD)95/dlg/ZO-1 (PDZ) domain–containing proteins, including cortactin-binding protein 1 (CortBP1) (Du et al., 1998), SHANK3 (Naisbitt et al., 1999), ZO-1 (Katsube et al., 1998), and an unrelated protein cortactin-binding protein (CBP-90) (Ohoka and Takai, 1998). Tyrosine phosphorylation of cortactin occurs in response to a wide variety of cellular events, including v-Src transformation (Wu et al., 1991), growth factor treatment (Maa et al., 1992; Zhan et al., 1993), bacterial invasion (Dehio et al., 1995; Fawaz et al., 1997), osmotic stress (Kapus et al., 1999), and integrin or syndecan-3 ligation with the extracellular matrix (Vuori and Ruoslahti, 1995; Kinnunen et al., 1998).

These previous studies suggest that cortactin plays an important role in coupling tyrosine kinase–based signaling events to cortical cytoskeletal reorganization. We have investigated the molecular mechanism by which cortactin interacts with the dynamic actin cytoskeleton. In this report we provide evidence that the Rac-induced localization of cortactin to the cell periphery requires two separate regions within the amino terminus: the amino-terminal acidic domain (NTA) and the fourth tandem repeat. We find that the fourth repeat is necessary for the F-actin binding activity of cortactin and that the NTA region binds directly to the Arp2/3 complex. Cortactin colocalizes with Arp2/3 complex at sites of dynamic actin assembly in lamellipodia. We propose that one of the roles of cortactin is to link PDZ-containing scaffolding proteins to sites of Arp2/3-mediated cortical actin assembly.

Materials and Methods

DNA Constructs

Cortactin expression constructs were created by PCR amplification of mp85.L7 (Miglarese et al., 1994). For production of cytomegalovirus (CMV)-driven cortactin constructs containing the FLAG epitope, the following cDNA fragments were produced by PCR: N-term (codons 1–330), NTA (codons 1–84), repeats (codons 85–330), and C-term (codons 350–546). All 5′ primers contained a KpnI restriction endonuclease site and all 3′ primers contained a stop codon followed by an EcoRI site. Amplified products were subcloned into KpnI-EcoRI–digested pcDNA3FLAG2AB (Devarajan et al., 1997). In some cases, PCR fragments were first cloned into PCR-Script (Stratagene) before subcloning. For construction of full-length cortactin lacking the fourth repeat, a KpnI-BamHI PCR fragment spanning the amino terminus to the end of the third repeat (codons 1–195) was ligated in frame with a BamHI-EcoRI fragment encoding the start of the fifth repeat through the carboxyl terminus (codons 232–546) and KpnI-EcoRI–digested pcDNA3FLAG2AB. The full-length FLAG-tagged cortactin construct has been described previously (Du et al., 1998).

CMV-driven myc-tagged cortactin expression constructs were produced by PCR as BamHI-EcoRI fragments and subcloned into BamHI-EcoRI–digested pRK5myc (Olson et al., 1996). Constructs produced were: full-length (codons 1–546), N-term (codons 1–330), N-repeat 5 (codons 1–269), N-repeat 4 (codons 1–232), N-repeat 3 (codons 1–195), N-repeat 2 (codons 1–158), N-repeat 1 (codons 1–121), repeat 3-C-term (codons 158–546), repeat 4-C-term (codons 195–546), repeat 5-C-term (codons 232–546), repeat 6-C-term (codons 269–546), and C-term (codons 350–546). FLAG-RacL61 was constructed by digestion of pRK5myc-RacL61 (Lamarche et al., 1996) with BamHI and EcoRI, and the resultant Rac cDNA fragment was subcloned into BamHI-EcoRI–digested pcDNA3FLAG2AB. Expression and immunoreactivity of each cortactin variant were verified by Western blotting of whole cell lysates with either the antiepitope tag mAbs M5 (against FLAG) or 9E10 (against myc) and anticortactin antibodies (data not shown).

For production of the glutathione *S*-transferase (GST)-cortactin prokaryotic expression constructs, GST-N-term, GST-NTA, and GST-repeats, BamHI-EcoRI PCR fragments were produced encoding the appropriate codons and subcloned into BamHI-EcoRI–digested pGST-parallel 2 (a gift from P. Sheffield, University of Virginia), as described previously (Sheffield et al., 1999). For the GST-N-repeat 5 construct, pRK5myc-N-repeat 5 was digested with BamHI and EcoRI and the cortactin fragment was subcloned into pGST-parallel 2. The GST construct containing the verpolin homology, cofilin, and acidic (VCA) domains of N-WASp has been described previously (Egile et al., 1999). All PCR-generated constructs were verified by DNA sequencing.

Antibodies and Western Blotting

The anticortactin antibodies anti-N-term, anti-C-term, and 4F11, have been described previously (Wu and Parsons, 1993; Weed et al., 1998). The specificity of the anti-N-term and C-term cortactin antibodies was verified by Western blotting of transfected cell lysates (see Fig. 1 B). The 9E10 mAb against the cmyc epitope was purchased from Santa Cruz Biotechnology, Inc. Anti-FLAG mAb M5 was purchased from Sigma-Aldrich. Affinity-purified rabbit pAbs against p21-Arc (Welch et al., 1997a) and Arp3 (a gift from M. Welch, University of California at Berkley, Berkeley, CA) (Welch et al., 1997b) were used for immunofluorescence detection of the Arp2/3 complex; rabbit antisera against Arp3, Arp2, and p34-Arc were used for Western blotting (a gift from L. Machesky, University of Birmingham, Birmingham, England) (Machesky et al., 1997). Fluorescently labeled secondary antibodies were purchased from Molecular

Probes, Jackson ImmunoResearch Laboratories, and CHEMICON International, Inc. Secondary antibodies coupled to horseradish peroxidase were purchased from Amersham Pharmacia Biotech.

Western blotting was performed as described previously (Kanner et al., 1990). Primary antibodies were used at the following concentrations or dilutions: 9E10 (3 μg/ml), M5 (5 μg/ml), 4F11 (1 μg/ml), anti-N-term or anti-C-term (1 μg/ml), Arp3 (1:500), and p34-Arc (1:500). Primary antibodies were detected with the appropriate horseradish peroxidase–conjugated secondary antibody (1:2,000) and immunoreactive bands were visualized using enhanced chemiluminescence (ECL; Amersham Pharmacia Biotech). Protein concentrations were determined using a bicinchonic acid assay kit (BCA; Pierce Chemical Co.).

Cell Culture, Microinjection, and Transfection

Swiss 3T3, C3H 10T1/2 (a gift from S. Parsons, University of Virginia), and PtK1 cells expressing a green fluorescent protein (GFP)-Arp3 fusion were cultured as described previously (Schafer et al., 1998; Weed et al., 1998). Subconfluent, serum-starved Swiss 3T3 cells were prepared as described (Lamarche et al., 1996). Microinjection of myc-tagged cortactin constructs and membrane ruffling initiated by PDGF and PMA were performed as described (Weed et al., 1998). At least 50 microinjected cells expressed each construct as determined by immunofluorescence microscopy. For transfection experiments, C3H 10T1/2 cells were grown to 80% confluence in 100-mm dishes and transfected with 10 μg of each epitope-tagged cortactin construct using SuperFect™ (QIAGEN). Cotransfection experiments with epitope-tagged RacL61 and cortactin constructs were conducted at a 4:1 (wt/wt) Rac/cortactin ratio. For immunofluoresence studies, cells were cultured 18 h after transfection, detached with trypsin/EDTA, neutralized with soybean trypsin inhibitor (Sigma-Aldrich), plated onto fibronectin-coated coverslips, and allowed to spread for 1 h, after which cells were fixed and processed for immunofluorescence microscopy. A minimum of 75 cotransfected cells was evaluated for each cortactin construct.

Immunofluoresence Microscopy

Swiss 3T3 and C3H 10T1/2 cells were fixed and immunolabeled as described (Weed et al., 1998). Epitope-tagged constructs were detected with either M5 (5 μg/ml) or 9E10 (3 μg/ml). Endogenous cortactin was labeled with either anti-N-term or anti-C-term (2 μg/ml). PtK1 cells were immunolabeled as described (Schafer et al., 1998). Cells were double labeled with the anticortactin mAb 4F11 (0.9 μg/ml) and anti-Arp3 (4 μg/ml) or p21-Arc (6 μg/ml). GFP-Arp3–expressing cells were labeled with 4F11.

Actin Cosedimentation Assays

F-actin binding assays were adapted from Fanning et al. (1998). Confluent 100-mm dishes of transfected C3H 10T1/2 cells were rinsed twice with PBS and collected on ice by scraping into 0.5 ml of binding buffer (10 mM imidazole, pH 7.2, 75 mM KCl, 5 mM $MgCl_2$, and 0.5 mM DTT) supplemented with 1 mM EGTA, 1 μg/ml leupeptin, and 1 μg/ml aprotinin. Cells were lysed with a Dounce homogenizer (50 strokes), and the lysate was centrifuged at 100,000 *g* for 1 h at 4°C. Rabbit muscle G-actin (Cytoskeleton) was diluted to 2.5 mg/ml in binding buffer and polymerized for 1 h at room temperature. F-actin (5.5 μM) was incubated with 60–80 μl of cell lysate (~50 μg of protein) in a final volume of 200 μl for 30 min at room temperature. Samples were centrifuged at 100,000 *g* for 1 h at 20°C in a 42.2 Ti rotor (Beckman Instruments), the supernatant was removed, and the pellet was incubated for 1 h at 4°C with 50 μl of G buffer (5 mM Tris-HCl, pH 8.0, 0.2 mM ATP, 0.5 mM DTT, and 0.2 mM $CaCl_2$) (Wu and Parsons, 1993). Supernatant and pellet fractions were normalized, and equal amounts were solublized in 2× SDS-PAGE sample buffer. Fractions were analyzed by SDS-PAGE and Western blotting with 4F11, M5, or 9E10 mAbs. Binding was quantitated by densitometric scans of the x-ray films shown in Figs. 3 and 4 for each immunoreactive band or an equivalent area from films exposed in a linear range using the program ImageQuant® (v.1.2; Molecular Dynamics). Percent bound was calculated as: $P/S + P \times 100$, where S and P are the amounts of cortactin immunoreactivity in the supernatant (S) and pellet (P) fraction.

Protein Preparation and Purification

GST-cortactin constructs were transformed into *Escherichia coli* strain DH5α, and fusion proteins were purified from isopropyl-1-thio-β-D-galactopyranoside–induced bacteria, as described (Sheffield et al., 1999). Fusion proteins were captured by incubation with glutathione–Sepharose 4B (5 ml/2 liters of culture; Amersham Pharmacia Biotech) and eluted with 10 mM reduced glutathione in suspension buffer (20 mM Tris-HCl, pH 8.0, 0.3 M NaCl, and 0.5 mM EDTA). TEV™ protease (300 U; GIBCO BRL) was added to the eluate, and the solution was dialyzed overnight at 4°C against 4 liters of suspension buffer containing 1 mM DTT. In cases of incomplete digestion, an additional 200 U of TEV™ was added, and the solution was incubated at 16°C overnight. Cleaved GST was removed by the addition of glutathione-Sepharose. TEV™ protease was removed by the addition of 200 μl of Ni-NTA™ agarose (50% slurry; QIAGEN). Arp2/3 complex was purified from bovine brain as described (Egile et al., 1999). Protein purity was monitored by Coomassie blue staining after SDS-PAGE, with all products estimated to be at least 90–95% pure.

Affinity Chromatography and Capillary Mass Spectrometry

Recombinant cortactin fragments (10 mg) were coupled to cyanogen bromide–activated Sepharose 4B (Amersham Pharmacia Biotech) according to the manufacturer's instructions. Resins were suspended in 1 ml of column buffer (20 mM Hepes-KOH, pH 7.8, 50 mM KCl, 1 mM EDTA, and 1% NP40) and stored at 4°C. Coupling efficiency was ~90%.

For affinity purification of amino-terminal cortactin binding proteins, extracts were initially prepared from murine brain. Whole brain tissue from 11 5–6-wk-old NIH 3T3 mice was Dounce homogenized in 8 ml of column buffer containing 10 mg/ml leupeptin and 1 mM PMSF. The lysate was centrifuged at 1,900 *g* for 10 min, and the supernatant was stored at −80°C. Cortactin N-term–Sepharose beads (100 μl of a 50% slurry containing ~1 mg of coupled protein) were incubated with 16 mg of brain lysate (4 mg/ml) for 30 min at 4°C. Beads were then washed with 4 ml of column buffer followed by 3 ml of column buffer containing 150 mM KCl. Bound proteins were eluted with 60 μl of SDS-PAGE sample buffer, separated by SDS-PAGE, and visualized by Coomassie blue staining or by Western blotting. Coomassie-stained bands representing proteins specifically associated with cortactin N-term were excised, trypsin digested, subjected to liquid chromatography mass spectrometry (LC-MS) analysis (Mandal et al., 1999), and analyzed by searching the NCBI database using a computer-based algorithm (Yates, 1998).

Additional experiments were performed using C3H 10T1/2 fibroblast lysate with an N-repeat 5 resin, since this protein was purified at much higher yields than cortactin N-term. Cells were lysed in column buffer containing inhibitors and centrifuged at 5,000 *g* for 5 min, and 3 mg of lysates (6 mg/ml) were incubated with 80 μl of GST, N-repeat 5, NTA, or repeats-Sepharose for 2 h at 4°C. After incubation, beads were washed twice with lysis buffer, and bound proteins were analyzed by Western blotting with anti-Arp3 antibodies.

Immunoprecipitation

C3H 10T1/2 cells transfected with FLAG-tagged cortactin constructs were lysed in lysis buffer supplemented with protease and phosphatase inhibitors (10 μg/ml leupeptin, 1.0 U/ml aprotinin, 0.5 mM PMSF, 0.5 mM EDTA, 1 mM sodium vanadate, and 40 mM sodium fluoride) and centrifuged at 5,000 *g* for 5 min. Clarified lysates (700 μg) were incubated with 20 μl of FLAG M2 affinity resin (Sigma-Aldrich) for 2 h at 4°C. Immune complexes were collected by centrifugation, washed twice with 1.0 ml of lysis buffer, separated by SDS-PAGE, and Western blotted with anti-Arp2, -Arp3, and -M5 antibodies.

Binding Assays

Arp2/3 complex (700 ng) was incubated with Sepharose conjugated to GST, cortactin NTA, cortactin N-repeat 5 or cortactin repeats 1–5 in 200 μl of binding buffer (20 mM Hepes, pH 7.5, 50 mM KCl, 1 mM EDTA, 0.1 mM ATP, 1% NP40) for 30 min at 4°C. The Sepharose was collected by centrifugation, washed twice with binding buffer without ATP, and bound Arp2/3 was visualized by Western blotting with anti-Arp3 after SDS-PAGE. For affinity measurements, 2.1 nM Arp2/3 was incubated with 0.46, 1.2, 2.3, and 4.7 μM cortactin N-repeat 5, as described above. The amount of Arp2/3 bound to cortactin was quantitated by densitometry and ImageQuant® as described above.

Actin Polymerization Assays

Actin polymerization assays were conducted essentially as described (Cooper et al., 1983). In brief, recombinant cortactin proteins (0.2–2.0 μM) or the GST-VCA fragment of human N-WASp (a gift from Marie-France Carlier, Dynamique du Cytosquelette, Laboratoire d'Enzymologie

et Biochemie Structurales, Gif-sur-Yvette, France) were incubated with 10 nM Arp2/3 complex in 20 mM imidazole, pH 7.0, 100 mM KCl, 2 mM $MgCl_2$, and 1 mM EGTA at 25°C. Actin polymerization was initiated by the addition of monomeric actin (7.5% pyrene labeled) and monitored by continuous measurement of the emission at 386 nm in a SPEX FluoroMax fluorometer (JY, Inc.). The temperature was maintained at 25°C throughout the experiment.

Results

Growth Factor–induced Translocation of Cortactin into Membrane Ruffles Requires the Amino-terminal Domain

In serum-starved cells, growth factor–mediated activation of Rac1 leads to the translocation of cortactin from cytoplasmic pools into lamellipodia, where it colocalizes with cortical F-actin (Weed et al., 1998). To identify the cortactin sequences necessary for lamellipodia localization, epitope-tagged cortactin expression constructs encoding various regions of the protein were introduced into mouse fibroblasts, and the Rac-induced translocation of the variant cortactin proteins to the cell cortex was evaluated (Fig. 1 A).

Subconfluent, serum-starved Swiss 3T3 fibroblasts were microinjected with either myc-N-term or myc-C-term constructs, and the intracellular distribution of N-term and C-term cortactin was compared with that of endogenous cortactin (Fig. 2). In serum-deprived cells, myc-N-term, myc-C-term, and endogenous cortactin were diffusely distributed throughout the cytoplasm (Fig. 2, A and B). Treatment of cells with PDGF or PMA, agents that activate Rac (Ridley et al., 1992), resulted in the accumulation of myc-N-term and endogenous cortactin within membrane ruffles at the cell cortex (Fig. 2 A). Myc-C-term cortactin failed to translocate efficiently to the cell periphery (Fig. 2 B). Therefore, the amino-terminal half of the cortactin molecule is necessary to target cortactin to the cell periphery.

Rac-induced Translocation of Cortactin to the Cell Cortex Requires Both the Amino-terminal Acidic and Tandem Repeat Region

To determine which region(s) within the amino-terminal domain are required for Rac-induced cortactin translocation, FLAG-tagged cortactin expression constructs were cotransfected with constitutively active myc-RacL61 into 10T1/2 fibroblasts. After plating on fibronectin for 1 h,

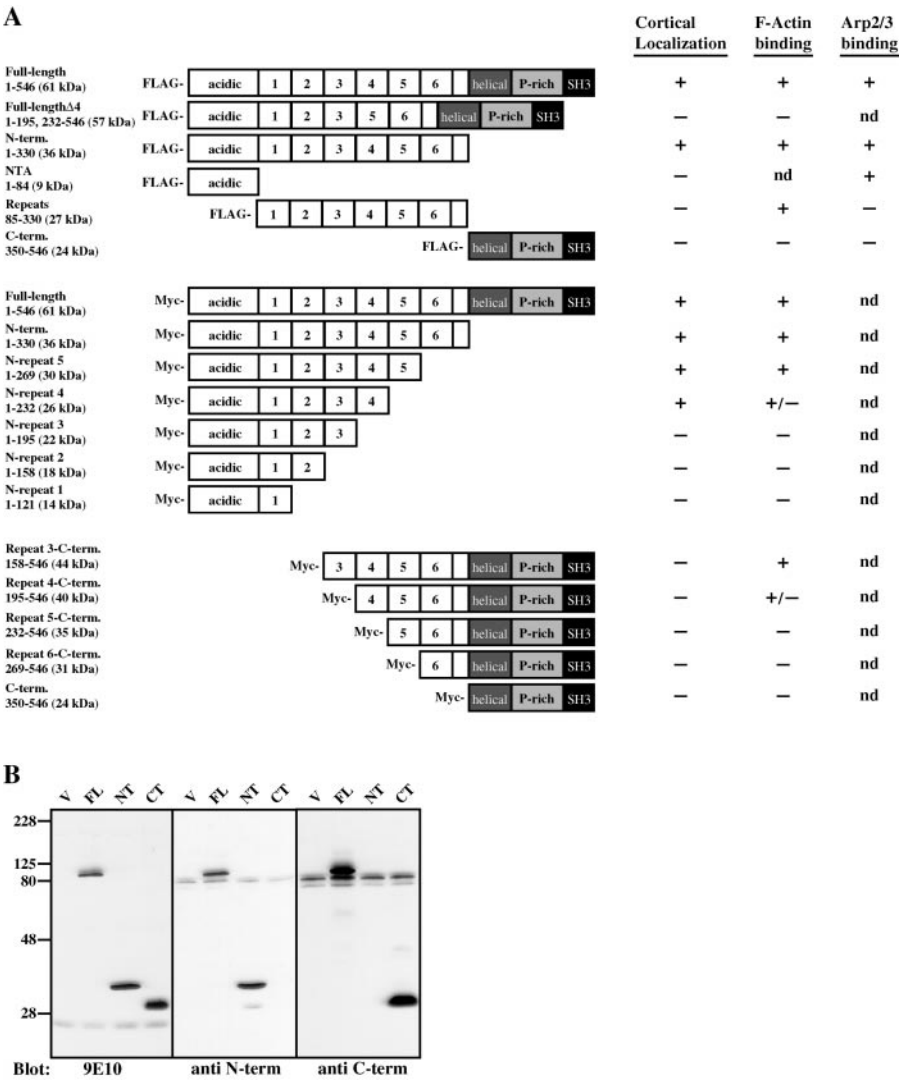

Figure 1. Cortactin variants and their activities. (A) Diagram of epitope-tagged cortactin expression constructs. Left: construct name, inclusive codons, and calculated molecular mass. Right: summary of Rac-induced localization, and F-actin and Arp2/3 binding properties. For cortical localization, a minimum of 50 microinjected or 75 transfected cells was assayed for each construct. +, at least 90% colabeling with endogenous translocated cortactin; −, 10% or less. For actin binding, + indicates 30–90% binding, +/− indicates 5–10%, and − indicates <2%. Arp 2/3 binding was evaluated by Western blotting for various Arp2/3 components (see Fig. 5). nd, not determined. (B) Validation of domain-specific anti-cortactin antibodies. 50 μg of C3H 10T1/2 lysate from cells transfected with either pRK5myc (V), myc-full-length (FL), myc-N-term (NT), or myc-C-term (CT) were subjected to SDS-PAGE and Western blotted with anti-myc (9E10), anti-N-term, or anti-C-term antibodies as indicated (bottom).

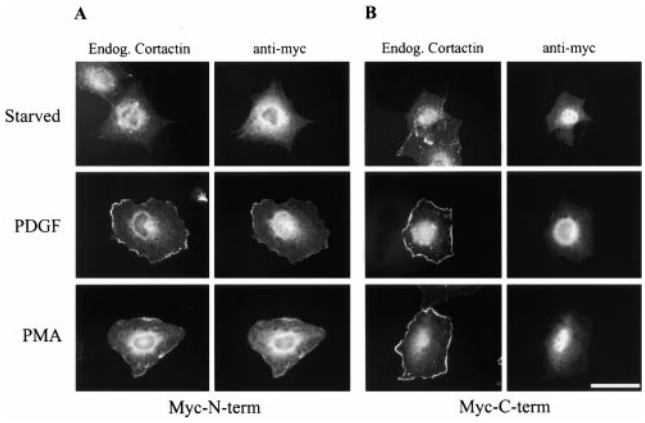

Figure 2. The cortactin amino-terminal domain is required for targeting to growth factor–induced membrane ruffles. Subconfluent, serum-starved Swiss 3T3 cells were microinjected with either myc-N-term (A) or myc-C-term (B). 2–3 h after microinjection, cells were left untreated (Starved) or treated with 5 ng/ml PDGF or 100 nM PMA as indicated. After stimulation, cells were fixed and coimmunostained for endogenous cortactin with anti-C-term (A) or anti-N-term (B) pAb and for expression of myc-tagged cortactin constructs with 9E10 (A and B). Bar, 50 μm.

cells expressing RacL61 were flat and round, with cortactin localized almost exclusively at the cell cortex (Fig. 3 A). FLAG-full-length cortactin and FLAG-N-term showed peripheral localization, whereas FLAG-C-term did not localize to the cortex, although endogenous cortactin did localize correctly (Fig. 3 B).

To further delineate the regions within the amino-terminal domain responsible for cortical targeting, FLAG-tagged constructs that encoded the NTA and the repeats domain (encompassing the six and one half tandem repeat sequences) were tested (Fig. 1 A). Both FLAG-NTA and FLAG-repeats failed to accumulate at the cell cortex when coexpressed with myc-RacL61, in spite of the near complete translocation of endogenous cortactin in cells expressing these constructs (Fig. 3 B). These data indicate that both the NTA and the repeat region are necessary for translocation of cortactin to the cell cortex, and that neither region alone is sufficient for translocation. Since the actin binding activity of cortactin is contained within the tandem repeat region (Wu and Parsons, 1993), cells expressing various FLAG-tagged cortactin constructs were lysed and the actin binding activity of the tagged cortactin constructs was evaluated (Fig. 3 C). FLAG-full-length and FLAG-N-term cosedimented with F-actin, whereas FLAG-C-term did not (Fig. 3 C). FLAG-repeats, which lacks the NTA region, bound actin at levels comparable to FLAG-N-term (Fig. 3 C). These data suggest that F-actin binding alone is insufficient for the peripheral localization of cortactin.

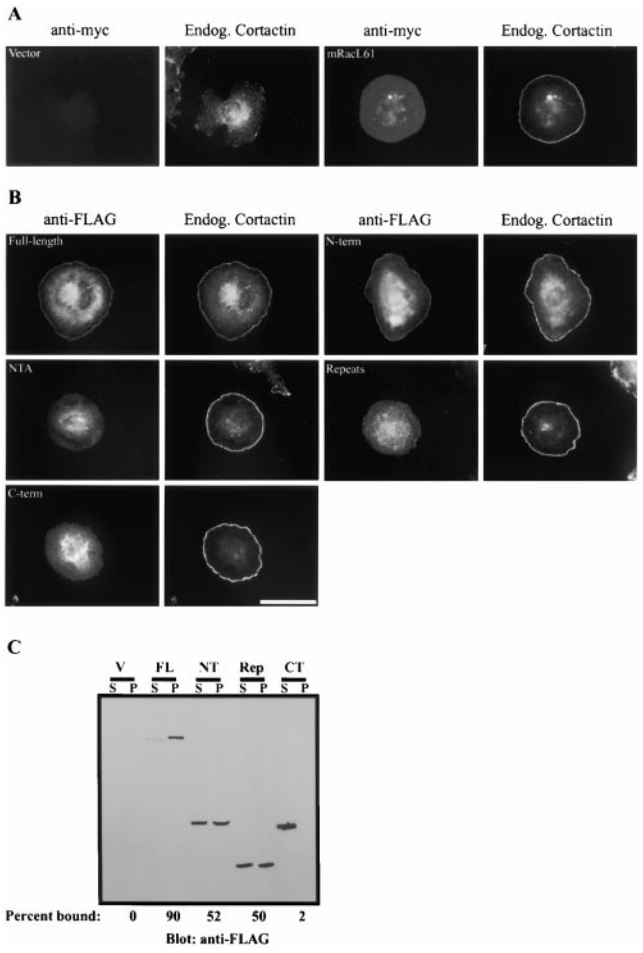

Figure 3. Cortical targeting of cortactin requires both the NTA and repeats region. (A) C3H 10T1/2 fibroblasts were transfected with pRK5myc or pRK5mycRacL61. Endog., endogenous cortactin. (B) Alternatively, cells were cotransfected with pRK5mycRacL61 and either FLAG-full-length, FLAG-N-term, FLAG-NTA, FLAG-repeats, or FLAG-C-term cortactin constructs. After transfection, cells were trypsinized, replated onto fibronectin-coated coverslips, and allowed to spread for 1 h before fixation. Cells were double labeled with 9E10 (A) or M5 (B) and either anti-C-term or anti-N-term cortactin antibodies. Bar, 50 μm. (C) The cortactin repeats region is required for F-actin binding. Lysates from C3H 10T1/2 cells transfected with pcDNA3FLAG2AB (V), FLAG-Full-length (FL), FLAG-N-term (NT), FLAG-repeats (Rep), and FLAG-C-term (CT) cortactin constructs were incubated with F-actin (5.5 μM). After centrifugation, supernatant (S) and pellet (P) fractions were resolved by SDS-PAGE and immunoblotted with the anti-FLAG mAb M5. The percentage of each cosedimented construct is indicated at the bottom (see Materials and Methods for further details). All constructs failed to sediment in the absence of F-actin (not shown).

The Fourth Cortactin Repeat Is Required for Cortical Localization and F-Actin Binding

The sequences of the six 37–amino acid tandem repeats in the cortactin amino terminus are highly similar to each other (Wu et al., 1991). To determine whether one or more of the tandem repeats was involved in cortical targeting, a series of myc-tagged cortactin expression constructs was produced that retained the NTA, but in which the individual tandem repeats were truncated from the carboxyl terminus of the myc-N-term construct (Fig. 1 A). Myc-N-term, Myc-N-repeat 5, and N-repeat 4 accumulated at the cell edge, but translocation of N-repeat 3, N-repeat 2, or N-repeat 1 (not shown) was significantly reduced (Fig. 4 A). These results suggest that the fourth repeat is required for cortical targeting. To directly test this, a full-length cortactin construct was produced lacking the fourth repeat (FLAG-full-lengthΔ4) and assayed for cortical localization, where it also failed to accumulate at the

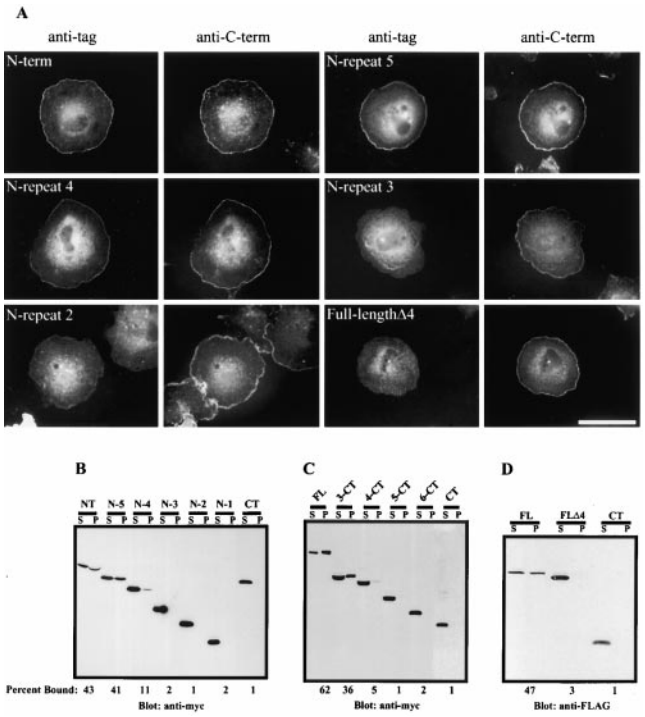

Figure 4. The fourth tandem repeat of cortactin is necessary for cortical localization and F-actin binding. (A) Repeat four is required for Rac-induced translocation. C3H 10T1/2 fibroblasts were cotransfected with FLAG-RacL61 and myc-N-term, myc-N-repeat 5, myc-N-repeat 4, myc-N-repeat 3, myc-N-repeat 2, and FLAG-Full-lengthΔ4 cortactin constructs. After trypsinization and replating onto fibronectin-coated coverslips, cells were double labeled with 9E10 and either anti-C-term or anti-N-term cortactin antibodies. Bar, 50 μm. (B–D) The fourth tandem repeat is central for the F-actin binding ability of cortactin. Lysates from C3H 10T1/2 cells transfected with myc-N-term (NT), myc-N-repeat 5 (N-5), myc-N-repeat 4 (N-4), myc-repeat 3 (N-3), myc-repeat 2 (N-2), myc-repeat 1 (N-1), myc-C-term (CT), myc-full-length (FL), myc-repeat 3-C-term (3-CT), myc-repeat 4-C-term (4-CT), myc-repeat 5-C-term (5-CT), myc-repeat 6-C-term (6-CT), c-term (CT), and FLAG-full-length (FL), FLAG-full-lengthΔ4 (FLΔ4), and FLAG-C-term (CT). Cortactin constructs were assayed for F-actin binding by cosedimentation and quantitated as described in the legend to Fig. 3. All constructs failed to sediment in the absence of F-actin (not shown).

cell periphery (Fig. 4 A). Endogenous cortactin translocated normally in all experiments. Taken together with the data presented above, we conclude that sequence elements within the fourth tandem repeat of cortactin are necessary for localization to the cell cortex.

Cortactin binds directly to F-actin with a K_d of 0.4 μM (Wu and Parsons, 1993), suggesting that targeting of cortactin to the leading edge may involve direct binding to cortical actin filaments. To define the portion of the repeat region responsible for actin binding, myc-N-term constructs containing serial deletions of individual repeats were assayed for F-actin binding in cell lysates (Fig. 4, B and C). Myc-N-term and myc-N-repeat 5 bound actin at comparable levels, whereas myc-N-repeat 4 bound actin at diminished levels (Fig. 4 B). Myc-N-repeat 3, myc-N-repeat 2, and myc-N-repeat 1 all failed to bind F-actin (Fig. 4 B). These data map the actin binding region of cortactin between the fourth complete and seventh partial tandem repeats. To further define which sequences within this region were required for actin binding, myc-tagged cortactin constructs were produced where the NTA and the individual tandem repeats were serially deleted from full-length cortactin beginning with the third repeat (Fig. 1 B). Myc-repeat 3-C-term displayed strong binding to F-actin, whereas myc-repeat 4-C-term weakly associated with F-actin (Fig. 4 C). Myc-repeat 5-C-term, myc-repeat 6-C-term, and myc-C-term all failed to significantly bind F-actin (Fig. 4 C). These data indicate that repeat four is central to the actin binding activity of cortactin, with efficient binding requiring a single adjacent repeat, either repeat three (Fig. 4 B) or repeat five (Fig. 4 C). The requirement for repeat four in actin binding was directly examined using FLAG-full-lengthΔ4, where removal of repeat four eliminated the binding of cortactin to F-actin (Fig. 4 D). These data, combined with the requirement for repeat four in cortical targeting, suggest that the ability of cortactin to localize with cortical actin networks in vivo requires the actin binding site located within the fourth tandem repeat.

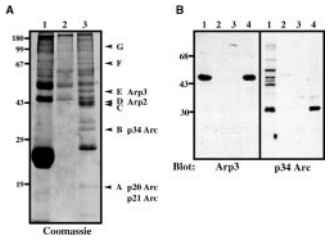

Figure 5. Association of the Arp2/3 complex with the cortactin amino terminus. (A) Identification of proteins interacting with the cortactin amino-terminal domain. Murine brain lysate was mixed with either GST-Sepharose (lane 1) or recombinant cortactin N-term–Sepharose (lane 3). Bound proteins were separated by SDS-PAGE and visualized by Coomassie blue staining. Bands representing proteins selectively associated with the cortactin amino-terminal domain (lane 3) were identified by comparison with the band profiles from GST-Sepharose (lane 1) and N-term–Sepharose incubated with elution buffer alone (lane 2). Proteins present in each selected band were sequenced as described in Materials and Methods. Positions of identified Arp2/3 complex proteins are indicated. Protein sequence coverage of all identified Arp2/3 components was at least 25%. p41-Arc and p16-Arc were not identified. (B) Immunoblotting of Arp2/3 components. Binding assays with cortactin N-term–Sepharose were conducted as described in A. After SDS-PAGE, proteins were Western blotted with antisera against Arp3 (left) and p34-Arc (right). Lane 1, 18 μg whole brain lysate; lane 2, GST-Sepharose incubated with lysate; lane 3, cortactin N-term–Sepharose incubated with binding buffer; lane 4, cortactin N-term–Sepharose incubated with lysate. The higher molecular weight products reactive against the p34-Arc antiserum present in whole brain lysate (lane 1) likely represent nonspecific binding to unknown proteins. Molecular weight markers are indicated in kD on the left.

The Cortactin Amino-terminal Domain Associates with the Arp2/3 Complex

Although the actin binding domain in repeat four is essential for cortical localization, the inability of the repeats region alone to target the cell cortex (Fig. 3 B) indicated that actin binding alone is insufficient for localization at the cell periphery. The NTA alone also failed to target to the cortex, but the NTA plus the repeats (i.e., N-term) did target appropriately. Therefore, we searched for other proteins that might interact with the amino-terminal domain and contribute to cortactin translocation. The cortactin

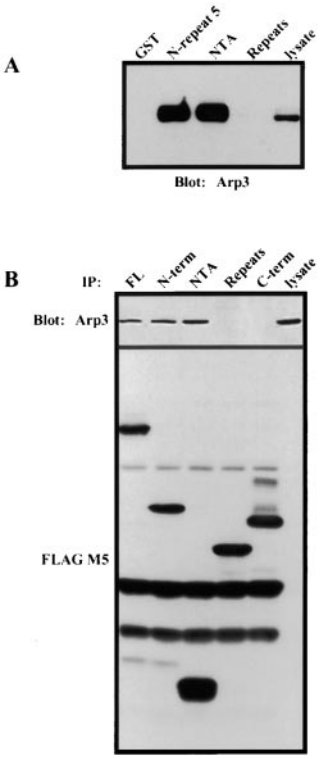

Figure 6. The Arp2/3 complex binds to the NTA region of cortactin. (A) C3H 10T1/2 cell lysate (3 mg) was incubated with GST-, cortactin N-repeat 5–, cortactin NTA-, and cortactin-repeats–Sepharose beads for 2 h, washed, and associated proteins were analyzed by Western blotting with Arp3 antisera. C3H 10T1/2 lysate (18 μg) was loaded as a positive control (right). (B) In vivo association of the Arp2/3 complex with the cortactin NTA region. C3H 10T1/2 cells transfected with FLAG-full-length (FL), FLAG-N-term, FLAG-NTA, FLAG-repeats, and FLAG-C-term cortactin constructs were immunoprecipitated with anti-FLAG resin. Immune complexes were washed, subjected to 10% SDS-PAGE, and analyzed for Arp2/3 association by Western blotting with Arp3 antisera (top). The blot was subsequently stripped, and expression of FLAG-cortactin constructs was verified by blotting with M5 (bottom). C3H 10T1/2 lysate (20 μg) was loaded as a control (rightmost lane).

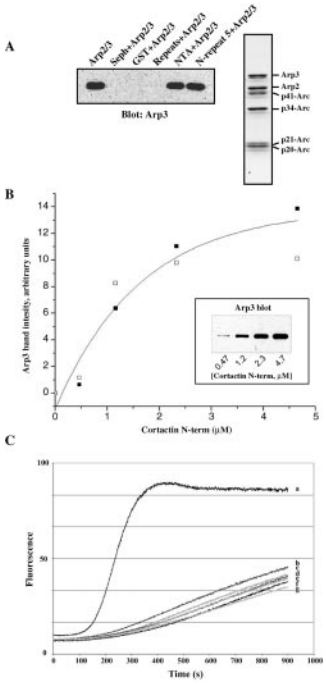

Figure 7. Cortactin interactions with the Arp2/3 complex. (A) Arp2/3 binds directly to the cortactin NTA region. Left panel: pure Arp2/3 complex (700 ng) was incubated with blank Sepharose (Seph+Arp2/3) or Sepharose conjugated to 30 μg GST (GST+Arp2/3), 60 μg cortactin repeats 1–5 (Repeats+Arp2/3), 30 μg cortactin NTA (NTA+Arp2/3), or 30 μg cortactin N-repeat 5 (N-repeat 5+Arp2/3). After incubation, the beads were washed and Arp2/3 binding was analyzed by Western blotting with Arp3 antisera. Purified Arp2/3 (140 ng) was loaded as a control (left). Right panel: Coomassie blue–stained SDS-PAGE analysis of purified Arp2/3 complex. (B) Affinity of Arp2/3 for cortactin. Purified Arp2/3 complex (2.1 nM) was incubated with 0.46, 1.2, 2.3, and 4.7 μM of cortactin N-repeat 5–Sepharose for 30 min, after which the complexes were washed and subjected to SDS-PAGE. Bound Arp2/3 complex was identified by Western blotting with Arp3 antisera, and Arp3 bands were quantitated by densitometry. The open and filled squares represent binding data from two independent experiments. An approximate K_d for binding was estimated to be 1.3 μM. Inset: representative Arp3 Western blot. (C) Functional analysis of cortactin–Arp2/3 interactions. Fluorometric measurement of actin polymerization was conducted with 2.5 μM G-actin (7.5% pyrene-labeled) and 10 nM Arp2/3 complex. Curves: (a) Arp2/3 + 5 nM GST-VCA fragment of N-WASp; (b) Arp2/3 + 0.5 μM cortactin N-repeat 5; (c) Arp2/3 + 0.5 μM cortactin repeats 1–5; (d) Arp2/3 + 0.5 μM GST-cortactin full-length; (e) Arp2/3 alone; (f) Arp2/3 + 0.5 μM cortactin NTA; (g) buffer.

amino-terminal domain was expressed in *E. coli* as a GST fusion protein, and the purified protein was covalently coupled to agarose beads. After application of a mouse brain extract, the affinity matrix was washed extensively and bound proteins were subjected to SDS-PAGE (Fig. 5 A). Based on a comparison with control lanes, 13 bands that appeared to represent proteins specifically associated with the cortactin amino-terminal domain were selected for LC-MS analysis. Sequence analysis and a search of the National Center for Biotechnology Information database revealed that four bands contained peptide sequences corresponding to five members of the Arp2/3 complex (Fig. 5 A). The presence of Arp2/3 complex proteins associated with N-term, but not control beads, was confirmed by Western blotting with antisera specific for Arp3 and p34Arc (Fig. 5 B). These data indicate that the Arp2/3 complex represents a subset of the proteins that interact with the amino terminus of cortactin.

Cortactin Binds the Arp2/3 Complex through Sequences in the NTA Region

To identify the region within the cortactin amino terminus responsible for associating with the Arp2/3 complex, Sepharose beads covalently coupled to the NTA and repeats regions were incubated with 10T1/2 fibroblast lysate, and Arp2/3 binding was assayed by immunoblotting (Fig. 6 A). Arp3 specifically bound to N-repeat 5 (see Materials and Methods) and NTA beads, but not to GST and repeats beads (Fig. 6 A), indicating that the NTA region is responsible for association with the Arp2/3 complex.

To confirm the interaction between cortactin and the Arp2/3 complex in vivo, 10T1/2 fibroblasts were transfected with FLAG-cortactin expression constructs, and overexpressed cortactin fusion proteins were immunoprecipitated with anti-FLAG. Coimmunoprecipitation of Arp2/3 complex proteins was assessed by immunoblotting. Both Arp3 (Fig. 6 B, top) and Arp2 (data not shown) coimmunoprecipitated with FLAG-full-length, FLAG-N-term, and FLAG-NTA. Precipitation of FLAG-repeats and FLAG-C-term fusion proteins failed to coprecipitate the Arp2/3 complex (Fig. 6 B). Precipitation of each FLAG-cortactin peptide was verified by immunoblotting with the anti-FLAG mAb M5 (Fig. 6 B, bottom). These data support the conclusion that cortactin interacts with the Arp2/3 complex through sequences within the 84–amino acid NTA domain.

Cortactin Binds to Purified Arp2/3 Complex: Functional Analysis of the Interactions

To determine whether the association of cortactin with Arp2/3 was direct, affinity chromatography assays were performed with various Sepharose-conjugated amino-terminal cortactin proteins and purified Arp2/3 complex (Fig. 7 A). Purified Arp2/3 complex bound to both NTA- and N-repeat 5–Sepharose but failed to bind to Sepharose

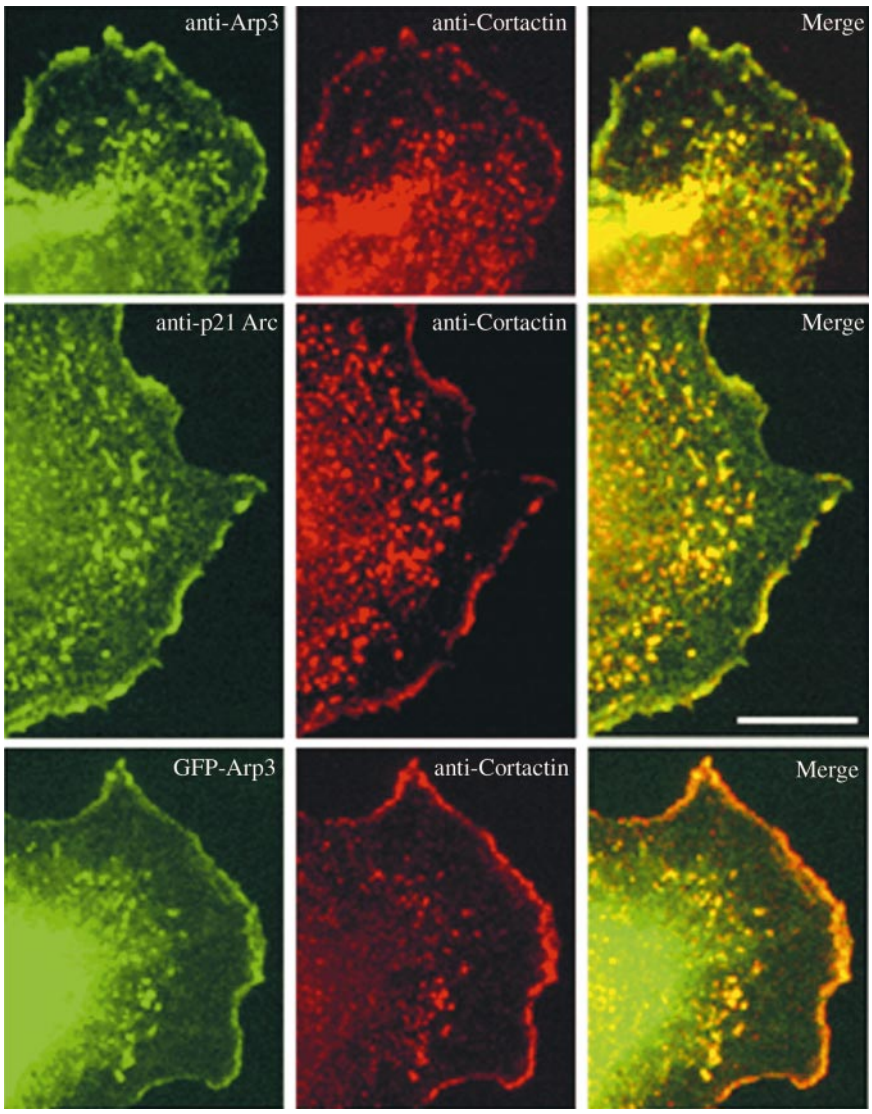

Figure 8. Colocalization of cortactin and the Arp2/3 complex in fibroblast lamellipodia. PtK1 fibroblasts cultured on poly-L-lysine–coated coverslips were fixed and colabeled using antibodies against either Arp3 (top) or p21-Arc (middle) with the anticortactin mAb 4F11. PtK1 cells expressing GFP-Arp3 (bottom) were labeled with 4F11. Merged image pairs demonstrate regions of overlap (yellow) between the Arp2/3 complex and cortactin at the leading edge and in peripheral punctate structures. Bar, 10 μm.

alone, GST, or repeat 1–5–Sepharose (Fig. 7 A). Furthermore, addition of increasing amounts of cortactin N-repeat 5-Sepharose to a fixed amount of Arp2/3 complex displayed saturable binding, with an estimated K_d of 1.3 μM (Fig. 7 B). These data strongly indicate that cortactin directly interacts with the Arp2/3 complex.

Since cortactin binds directly to Arp2/3 complex, we hypothesized that cortactin might stimulate the actin nucleation activity of Arp2/3. Stimulation of Arp2/3 complex was measured in a pyrene actin polymerization assay (Fig. 7 C). Nucleation of new actin filaments by Arp2/3 complex causes a rapid rise in pyrene actin fluorescence due to the increased number of free barbed ends available for polymerization (Higgs et al., 1999). In the presence of 10 nM Arp2/3 complex and 2.5 μM actin, cortactin N-repeat 5 (curve b), repeat 1–5 (curve c), full-length (curve d), and NTA (curve f) (all at 0.5 μM) failed to stimulate Arp2/3 complex to nucleate new actin filaments (Fig. 7 C). Concentrations of cortactin proteins up to 1 μM did not activate the Arp2/3 complex (n = 3, data not shown). Addition of the N-WASp VCA domain (curve a) strongly promoted actin nucleation, indicating that the Arp2/3 complex was functional. Also, cortactin proteins, at concentrations up to 2 μM, did not inhibit the ability of the VCA fragment at threshold (0.5 nM) concentrations to activate Arp2/3 complex. When the concentration of the Arp2/3 complex was increased 10-fold to 100 nM, cortactin at 0.5 μM showed weak activation of nucleation. The nature of the weak cortactin-dependent nucleation activity is currently under study.

Cortactin Localizes with the Arp2/3 Complex in Fibroblast Lamellipodia

To determine if cortactin and the Arp2/3 complex were present within the same subcellular compartments, cortactin and Arp2/3 complex localization in fibroblast lamellipodia was determined by indirect immunofluoresence. Double staining of PtK1 cells with antibodies specific for Arp3 or p21-Arc (Welch et al., 1997a) and the anticortactin mAb 4F11 (Fig. 8) yielded very similar staining patterns, with both components being present at the leading edge and in peripheral spots (Schafer et al., 1998). Merged images demonstrated a large degree of overlap in both subcellular regions. Colocalization of cortactin with Arp3 was also demonstrated in a PtK1 cell line stably expressing GFP-Arp3 (Schafer et al., 1998). GFP-Arp3 and cortactin

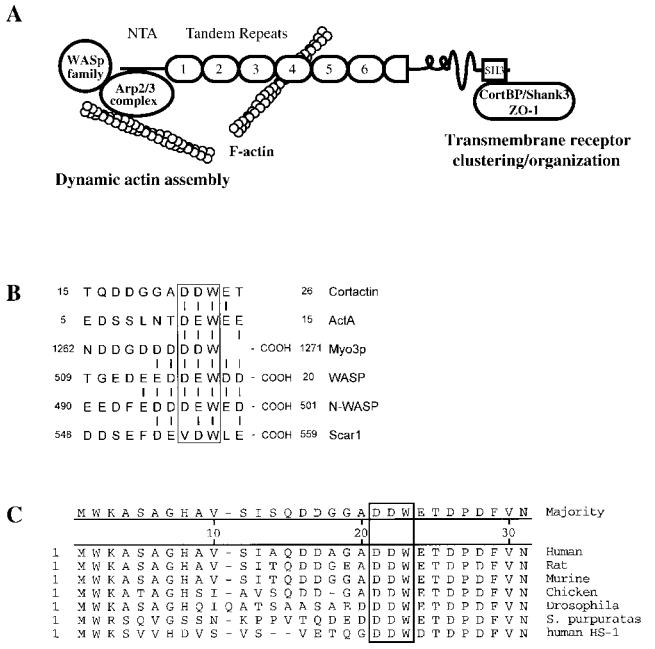

Figure 9. Cortactin links transmembrane receptor complexes to sites of dynamic actin assembly. (A) Diagram of cortactin binding proteins. Arp2/3 complex–WASp/Scar are depicted binding to the NTA. Binding of cortactin to F-actin through sequences in the fourth tandem repeat tethers cortactin to polymerized actin. The SH3 domain of cortactin binds the PDZ-containing proteins CortBP1/SHANK and ZO-1. The role of these interactions are discussed in the text. (B) Comparison of cortactin NTA with interaction motifs in Arp2/3 binding proteins. The acidic interaction domain of reported Arp2/3-activating proteins contain either a DDW or DEW sequence (boxed, except Scar1) within or near their demonstrated Arp2/3 binding regions. The NTA region of cortactin also contains this motif, which may confer the ability to bind to and/or activate Arp2/3 complex. Aligned sequences shown are from Miglarese et al. (1994) (cortactin), Wiedmann et al. (1997) (ActA), Dujon et al. (1994) (Myo3p), Derry et al. (1995) (WASp), Fukuoka et al. (1997) (N-WASp), and Bear et al. (1998) (Scar1). Numbers indicate the position of flanking residues. (C) The cortactin DDW motif is conserved among different species. Alignment of the first 30–32 amino acids of human (sequence data available from EMBL/GenBank/DDBJ under accession no. M98343), rat (AF054619), murine (U03184), chicken (M73705), *Drosophila* (AB009998), *Strongylocentrotus purpuratus* (AF064260), and human HS-1 (X16663) cortactin. The DDW motif is boxed; consensus resides are shown at the top (Majority).

were both present at the leading edge and within peripheral spots, with significant overlap in merged images (Fig. 8). Based on these data, we conclude that cortactin is a component of the Arp2/3-regulated cortical actin structures present in lamellipodia.

Discussion

Cortactin is involved in several protein tyrosine kinase–based signaling pathways, where its phosphorylation is coincident with reorganization of cortical actin cytoskeletal networks. The localization of cortactin with cortical F-actin within lamellipodia requires Rac activity (Weed et al., 1998). The sequences responsible for the selective targeting of cortactin to the cell periphery are unknown. In this report we provide evidence that Rac-induced localization of cortactin to the cell cortex requires two distinct sequence motifs within the amino-terminal half of the protein. One targeting motif encompasses the fourth 37–amino acid tandem repeat. Removal of repeat four abolishes the ability of cortactin to localize at the cell periphery in cells cotransfected with RacL61 and greatly diminishes binding of cortactin to F-actin in vitro. The second localization motif resides within the 84–amino acid NTA region and is also required for Rac-induced cortical localization. The NTA region binds to the Arp2/3 complex as determined by affinity chromatography and immunoprecipitation from cell lysates and by direct binding assays with purified cortactin and the Arp2/3 complex. Immunofluoresence localization experiments support a functional interaction between cortactin and the Arp2/3 complex in that the Arp2/3 complex and cortactin colocalize at the leading edge and within punctate spots within lamellipodia, both regions of active actin dynamics. Therefore, we conclude that the Rac-induced interaction of cortactin with cortical sites of actin assembly requires the bipartite interaction of cortactin with actin filaments and the Arp2/3 complex (Fig. 9 A).

Cortactin interacts with components of the cortical actin network in several cell types. In addition to the lamellipodia of cultured cells (Wu and Parsons, 1993; Weed et al., 1998), cortactin is also found at sites of cortical F-actin reorganization in many differentiated cells, including growth cones and the PSD of neurons (Du et al., 1998; Naisbitt et al., 1999), the terminal web of polarized epithelia (Wu and Montone, 1998), and neuromuscular junctions (Peng et al., 1997). The biochemical mechanism discussed here, in which cortactin interacts with both F-actin and the Arp2/3 complex, may also be the basis for the interaction of cortactin with dynamic actin in these other specialized cellular compartments.

Regulation of the actin cytoskeleton plays an essential role in the organization of transmembrane receptor complexes within highly specialized cell structures (Bloch and Morrow, 1989; Adam and Matus, 1996; Jou et al., 1998). The data presented in this report, in conjunction with the characterization of several cortactin SH3 domain binding proteins, leads us to propose that cortactin functions to link a variety of cell surface receptors to sites of Arp2/3-directed actin polymerization (Fig. 9 A). In neurons, the SH3 domain of cortactin interacts with members of the CortBP1/SHANK family of scaffolding proteins (Du et al., 1998; Naisbitt et al., 1999). CortBP1/SHANK proteins possess a single PDZ domain and are capable of interacting directly with the type 2 somatostatin receptor (Zitzer et al., 1999) or indirectly through the scaffolding proteins guanylate kinase–associated protein (GKAP), PSD95, or Homer to the *N*-methyl-D-aspartate (NMDA), inositiol trisphosphate, or metabotropic glutamate receptors (Boeckers et al., 1999; Naisbitt et al., 1999; Tu et al., 1999). Additionally, the SH3 domain of cortactin binds ZO-1, a component of tight junctions (Katsube et al., 1998). Tight junctions occur in the terminal web of polarized epithelia (Fath et al., 1993), a region where ZO-1 and cortactin are colocalized (Stevenson et al., 1986; Wu and Montone, 1998). ZO-1 is structurally similar to PSD-95 (Itoh et al., 1993) and has been implicated in regulating tight junction assembly (Sheth et al., 1997). ZO-1 binds to cytoplasmic motifs in occludin (Furuse et al., 1994) and claudin (Itoh et

al., 1999), two transmembrane proteins implicated in forming the paracellular seal between adjacent cells (Furuse et al., 1998). Therefore, the coupling of ZO-1 to Arp2/3-mediated actin dynamics by cortactin may in part contribute to the organization and assembly of transmembrane networks within tight junctions as well as at the PSD (Fig. 9 A).

Activation of the Arp2/3 complex has been suggested to be critical for protrusive-based actin locomotion (Borisy and Svitkina, 2000). Colocalization of cortactin with the Arp2/3 complex at the leading edge and in protrusive distal lamellar regions (Schafer et al., 1998), the direct binding of cortactin to Arp2/3 in vitro, and the tyrosine phosphorylation of cortactin in response to growth factor receptor activation (Maa et al., 1992; Zhan et al., 1993) suggest a role for cortactin in linking sites of actin polymerization to cell surface receptor complexes. The observation that cortactin does not efficiently stimulate Arp2/3-dependent actin nucleation (although low levels of nucleation are observed at higher concentrations of Arp2/3) is consistent with cortactin not being a direct activator of actin polymerization. However, it is possible that additional factors/proteins may cooperate to increase the effect of cortactin on Arp2/3 activation.

Thus, possible functions of cortactin may be to bridge sites of dynamic actin reorganization with receptor signaling complexes and/or to recruit, via SH3 interactions, other proteins that may positively or negatively regulate Arp2/3 actin polymerization.

In addition to WASp/Scar family proteins, binding of ActA from *Listeria monocytogenes* (Welch et al., 1998) or yeast Myo3p and 5p (Evangelista et al., 2000; Lechler et al., 2000) stimulates actin reorganization mediated entirely, or in part, by the Arp2/3 complex. Whereas carboxyl-terminal acidic regions from WASp and Scar bind to p21-Arc (Machesky and Insall, 1998), Myo3p and 5p bind Arc40p (equivalent to mammalian p41-Arc) through the carboxyl-terminal tryptophan residue (Evangelista et al., 2000). The cortactin NTA region contains a sequence motif (DDW) that is identical to the last three amino acids in Myo3 and Myo5p, and homologous sequences are present in the carboxyl terminus of nearly all WASp/Scar family proteins (Fig. 9 B). The ActA amino terminus contains a similar motif near sequence elements required for the maintenance of *Listeria* actin tail formation (Lasa et al., 1997). This sequence in cortactin is conserved across species and is also present in the cortactin-related protein HS1 (Fig. 9 C). We are currently testing if this motif is required for the binding of cortactin to the Arp2/3 complex.

The data presented here indicate that the fourth tandem repeat is necessary for the F-actin binding activity of cortactin and for targeting cortactin to cortical actin structures. The sequence of repeat four is not homologous to other actin binding domains. Isoforms of cortactin are generated by alternative splicing, with cortactin A (Ohoka and Takai, 1998) corresponding to the full-length cortactin form used in these studies. Alternative splicing removes repeat six (cortactin B) or repeats 5 and 6 (cortactin C); all of these isoforms bind F-actin. These results, coupled with the reported inability of the first three cortactin repeats to bind F-actin (He et al., 1998), support the conclusion that the F-actin binding domain is contained within repeat four. Cortactin variants containing the sixth repeat are reported to cross-link F-actin (Huang et al., 1997; Ohoka and Takai, 1998), an activity that can be downregulated by Src-mediated phosphorylation of cortactin (Huang et al., 1997). Furthermore, based on the analysis of the cortactin-related protein HS1 (Kitamura et al., 1989) and HS1–cortactin hybrid proteins, the fourth cortactin tandem repeat has been suggested to interact with phosphatidylinositol 4,5-bisphosphate (PIP_2), which also downregulates F-actin cross-linking by cortactin (He et al., 1998). In spite of these data, the mechanism by which cortactin cross-links actin filaments is currently unknown.

The association of cortactin with the Arp2/3 complex and F-actin is likely to impact multiple signaling pathways in a variety of cell types. In addition to linking scaffolding proteins in neuronal and epithelial systems, cortactin may also link the machinery for actin polymerization, Arp2/3 complexes, to signals emanating from the leading edge of motile cells. Ectopic overexpression of cortactin stimulates cell motility that is dependent on Src phosphorylation (Huang et al., 1998; Patel et al., 1998), suggesting that cortactin contributes to cell migration mediated by Src kinase activity (LaVallee et al., 1998; Liu et al., 1999). Cortactin is overexpressed in many cell lines derived from human tumors containing amplification of chromosome 11q13 that posses high metastatic potential (Schuuring et al., 1992; Patel et al., 1996) and is present within invadopodia in invasive breast cancer cell lines (Bowden et al., 1999). Invadopodia serve as sites of extracellular matrix degradation by sequestering or secreting various serine and metalloproteinases (Chen and Wang, 1999), and such structures directly correlate with invasive potential. How cortactin overexpression leads to increased motility and metastatic potential is currently unclear.

The proper spatial and temporal localization of cortactin with newly forming cortical actin networks is likely to be important for cortactin function. Recently, it was shown that the activity of Rac and the EGF receptor synergize to enhance signaling to the Raf-Mek-Erk pathway leading to cell motility (Leng et al., 1999). Therefore, Rac-induced localization of cortactin at sites of Arp2/3 activity may enhance the efficiency of signal transmission at the leading edge by linking growth factor–mediated receptor signals to downstream effector pathways (Klemke, et al., 1997). Activated Arp2/3 complex forms a polarized gradient during neutrophil chemotaxis, becoming concentrated at the migratory front (Weiner et al., 1999), and is coincident with sites of activation of chemoattractant receptor signaling complexes (Servant et al., 2000). Organization of receptor signaling complexes at the leading edge may in part be controlled by Arp2/3 and/or cortactin. EGF-induced cell motility also requires the integration of multiple signaling pathways (Wells et al., 1998). Tyrosine phosphorylation of cortactin initiated by EGF (Maa et al., 1992), in conjunction with the distribution of cortactin with dynamic cortical actin structures, positions cortactin as a potential mediator of one or more of these signaling pathways. The possibility that cortactin plays a role in the regulation of cortical actin assembly and/or spatial organization of cell surface receptors suggests that cortactin may provide an important site of signal integration between protein tyrosine kinases and the actin cytoskeleton.

We thank Nicholas Sherman and Jay Fox (W.M. Keck Biomedical Mass Spectrometry Laboratory, University of Virginia) for mass spectrometry analysis, and Alan Fanning (Yale University, New Haven, CT) for advice on actin binding assays.

This work was support by grants CA40042 and CA29243 from the Department of Health and Human Services-National Institutes of Health (NIH)/National Cancer Institute to J.T. Parsons and by NIH grant GM38542 to J.A. Cooper. S.A. Weed is supported by NIH postdoctoral fellowship CA75695. The University of Virginia Biomolecular Research Facility is funded by a grant from the University of Virginia Pratt Committee.

Submitted: 18 April 2000
Revised: 17 August 2000
Accepted: 23 August 2000

Note added in proof. Mutation of the DDW motif in the NTA region significantly reduced the in vitro binding of Arp2/3 to NTA-Sepharose.

References

Adam, G., and A. Matus. 1996. Role of actin in the organisation of brain postsynaptic densities. *Brain Res. Mol. Brain Res*. 43:246–250.

Ayscough, K.R. 1998. In vivo functions of actin-binding proteins. *Curr. Opin. Cell Biol.* 10:102–111.

Bear, J.E., J.F. Rawls, and C.L. Saxe. 1998. SCAR, a WASP-related protein, isolated as a suppressor of receptor defects in late *Dictyostelium* development. *J. Cell Biol.* 142:1325–1335.

Bi, E., and S.H. Zigmond. 1999. Actin polymerization: where the WASP stings. *Curr. Biol.* 9:R160–R163.

Bloch, R.J., and J.S. Morrow. 1989. An unusual beta-spectrin associated with clustered acetylcholine receptors. *J. Cell Biol.* 108:481–493.

Boeckers, T.M., C. Winter, K.-H. Smalla, M.R. Kreutz, J. Bockmann, C. Seidenbecher, C.C. Garner, and E.D. Gundelfinger. 1999. Proline-rich synapse-associated proteins ProSAP1 and ProSAP2 interact with synaptic proteins of the SAPAP/GKAP family. *Biochem. Biophys. Res. Commun.* 264: 247–252.

Borisy, G.G., and T.M. Svitkina. 2000. Actin machinery: pushing the envelope. *Curr. Opin. Cell Biol.* 12:104–112.

Bowden, E.T., M. Barth, D. Thomas, R.I. Glazer, and S.C. Mueller. 1999. An invasion-related complex of cortactin, paxillin and PKCμ associates with invadopodia at sites of extracellular matrix degradation. *Oncogene.* 18:4440–4449.

Chan, A.Y., S. Raft, M. Bailly, J.B. Wyckoff, J.E. Segall, and J.S. Condeelis. 1998. EGF stimulates an increase in actin nucleation and filament number at the leading edge of the lamellipod in mammary adenocarcinoma cells. *J. Cell Sci.* 111:199–211.

Chen, W.T., and J.Y. Wang. 1999. Specialized surface protrusions of invasive cells, invadopodia and lamellipodia, have differential MT1-MMP, MMP-2, and TIMP-2 localization. *Ann. NY Acad. Sci.* 878:361–371.

Cooper, J.A., S.B. Walker, and T.D. Pollard. 1983. Pyrene actin: documentation of the validity of a sensitive assay for actin polymerization. *J. Muscle Res. Cell Motil.* 4:253–262.

Dehio, C., M.-C. Prevost, and P.J. Sansonetti. 1995. Invasion of epithelial cells by *Shigella flexneri* induces tyrosine phosphorylation of cortactin by a $pp60^{c\text{-}src}$-mediated signalling pathway. *EMBO (Eur. Mol. Biol. Organ.) J.* 14:2471–2482.

Derry, J.M., P. Wiedemann, P. Blair, Y. Wang, J.A. Kerns, V. Lemahieu, V.L. Godfrey, J.E. Wilkinson, and U. Francke. 1995. The mouse homolog of the Wiskott-Aldrich syndrome protein (WASP) gene is highly conserved and maps near the scurfy (sf) mutation on the X chromosome. *Genomics.* 29: 471–477.

Devarajan, P., P.R. Stabach, M.A. Dematteis, and J.S. Morrow. 1997. Na,K-ATPase transport from endoplasmic reticulum to Golgi requires the Golgi spectrin-ankyrin G119 skeleton in Madin-Darby canine kidney cells. *Proc. Natl. Acad. Sci. USA*. 94:10711–10716.

Du, Y., S.A. Weed, W.-C. Xoing, T.D. Marshall, and J.T. Parsons. 1998. Identification of a novel cortactin SH3 domain-binding protein and its localization to growth cones of cultured neurons. *Mol. Cell. Biol.* 18:5838–5851.

Dujon, B., D. Alexandraki, B. Andre, W. Ansorge, V. Baladron, J.P. Ballesta, A. Banreve, P.A. Bolle, M. Bolotin-Fukuhara, and P. Bossier, et al. 1994. Complete DNA sequence of yeast chromosome XI. *Nature.* 369:371–378.

Egile, C., T.P. Loisel, V. Laurent, R. Li, D. Pantaloni, P.J. Sansonetti, and M.-F. Carlier. 1999. Activation of the Cdc42 effector N-WASP by the *Shigella flexneri* IcsA protein promotes actin nucleation by Arp2/3 complex and bacterial actin-based motility. *J. Cell Biol.* 146:1319–1332.

Evangelista, M., B.M. Klebl, A.H.Y. Tong, B.A. Webb, T. Leeuw, E. Leberer, M. Whiteway, D.Y. Thomas, and C. Boone. 2000. A role for myosin-I in actin assembly through interactions with Vrp1p, Bee1p, and the Arp2/3 complex. *J. Cell Biol.* 148:353–362.

Fanning, A.S., B.J. Jameson, L.A. Jesaitis, and J.M. Anderson. 1998. The tight junction protein ZO-1 establishes a link between the transmembrane protein occludin and the actin cytoskeleton. *J. Biol. Chem.* 273:29745–29753.

Fath, K.R., S.N. Mamajiwalla, and D.R. Burgess. 1993. The cytoskeleton in development of epithelial cell polarity. *J. Cell Sci. Suppl.* 17:65–73.

Fawaz, F.S., C. van Ooij, E. Homola, S.C. Mutka, and J.N. Engel. 1997. Infection with *Chlamydia trachomatis* alters the tyrosine phosphorylation and/or localization of several host cell proteins including cortactin. *Infect. Immun.* 65:5301–5308.

Fukuoka, M., H. Miki, and T. Takenawa. 1997. Identification of N-WASP homologs in human and rat brain. *Gene.* 196:43–48.

Furuse, M., M. Itoh, T. Hirase, A. Nagafuchi, S. Yonemura, S. Tsukita, and S. Tsukita. 1994. Direct association of occludin with ZO-1 and its possible involvement in the localization of occludin at tight junctions. *J. Cell Biol.* 127: 1617–1626.

Furuse, M., H. Sasaki, K. Fujimoto, and S. Tsukita. 1998. A single gene product, claudin-1 or -2, reconstitutes tight junction strands and recruits occludin in fibroblasts. *J. Cell Biol.* 143:391–401.

Hall, A. 1998. Rho GTPases and the actin cytoskeleton. *Science.* 279:509–514.

He, H., T. Watanabe, X. Zhan, C. Huang, E. Schuuring, K. Fukami, T. Takenawa, C.C. Kumar, R.J. Simpson, and H. Maruta. 1998. Role of phosphatidylinositol 4,5-bisphosphate in Ras/Rac-induced disruption of the cortactin-actomyosin II complex and malignant transformation. *Mol. Cell. Biol.* 18: 3829–3837.

Higgs, H.N., and T.D. Pollard. 1999. Regulation of actin polymerization by Arp2/3 complex and WASp/Scar proteins. *J. Biol. Chem.* 274:32531–32534.

Higgs, H.N., L. Blanchion, and T.D. Pollard. 1999. Influence of the C terminus of Wiskott-Aldrich Syndrome protein (WASp) and the Arp2/3 complex on actin polymerization. *Biochemistry.* 38:15212–15222.

Huang, C., Y. Ni, Y. Gao, C.C. Haundenschild, and X. Zhan. 1997. Down-regulation of the filamentous actin cross-linking activity of cortactin by Src-mediated tyrosine phosphorylation. *J. Biol. Chem.* 272:13911–13915.

Huang, C., J. Liu, C.C. Haudenschild, and X. Zhan. 1998. The role of tyrosine phosphorylation of cortactin in the locomotion of endothelial cells. *J. Biol. Chem.* 273:25770–25776.

Itoh, M., A. Nagafuchi, S. Yonemura, T. Kitani-Yasuda, S. Tsukita, and S. Tsukita. 1993. The 220-kD protein colocalizing with cadherins in non-epithelial cells is identical to ZO-1, a tight junction–associated protein in epithelial cells: cDNA cloning and immunoelectron microscopy. *J. Cell Biol.* 121:491–502.

Itoh, M., M. Furuse, K. Morita, K. Kubota, M. Saitou, and S. Tsukita. 1999. Direct binding of three tight junction–associated MAGUKs, ZO-1, ZO-2, and ZO-3, with the COOH termini of claudins. *J. Cell Biol.* 147:1351–1363.

Jou, T.-S., E.E. Schneegerger, and W.J. Nelson. 1998. Structural and functional regulation of tight junctions by RhoA and Rac1 small GTPases. *J. Cell Biol.* 142:101–115.

Kanner, S.B., A.B. Reynolds, R.R. Vines, and J.T. Parsons. 1990. Monoclonal antibodies to individual tyrosine-phosphorylated protein substrates of oncogene-encoded tyrosine kinases. *Proc. Natl. Acad. Sci. USA.* 87:3328–3332.

Kapus, A., K. Szaszi, J. Sun, S. Rizoli, and O.D. Rotstein. 1999. Cell shrinkage regulates src kinases and induces tyrosine phosphorylation of cortactin, independent of the osmotic regulation of Na^+/H^+ exchangers. *J. Biol. Chem.* 274:8093–8102.

Katsube, T., M. Takahisa, R. Ueda, N. Hashimoto, M. Kobayashi, and S. Togashi. 1998. Cortactin associates with the cell–cell junction protein ZO-1 in both *Drosophila* and mouse. *J. Biol. Chem.* 273:29672–29677.

Kessels, M.M., A.E. Engqvist-Goldstein, and D.G. Drubin. 2000. Association of mouse actin-binding protein 1 (mAbp1/SH3P7), an src kinase target, with dynamic regions of the cortical actin cytoskeleton in response to Rac1 activation. *Mol. Biol. Cell.* 11:393–412.

Kinnunen, T., M. Kaksonen, J. Saarinen, N. Kalkkinen, H.B. Peng, and H. Rauvala. 1998. Cortactin-Src kinase signaling pathway is involved in N-syndecan-dependent neurite outgrowth. *J. Biol. Chem.* 273:10702–10708.

Kitamura, D., H. Kaneko, Y. Miyagoe, T. Ariyase, and T. Wantanabe. 1989. Isolation and characterization of a novel human gene expressed specifically in cells of hemopoietic lineage. *Nucleic Acids Res.* 17:9367–9379.

Klemke, R.L., S. Cai, A.L. Giannini, P.J. Gallagher, P. de Lanerolle, and D.A. Cheresh. 1997. Regulation of cell motility by mitogen-activated protein kinase. *J. Cell Biol.* 137:481–492.

Kobayashi, K., S. Kuroda, M. Fukata, T. Nakamura, T. Nagase, N. Nomura, Y. Matsuura, N. Yoshida-Kubomura, A. Iwamatsu, and K. Kaibuchi. 1998. P140Sra-1 (specifically Rac1-associated protein) is a novel specific target for Rac1 small GTPase. *J. Biol. Chem*. 273:291–295.

Kozma, R.,S. Ahmed, A. Best, and L. Lim. 1995. The ras-related protein cdc42Hs and bradykinin promote formation of peripheral actin microspikes and filopodia in Swiss 3T3 fibroblasts. *Mol. Cell. Biol.* 15:1942–1952.

Lamarche, N., N. Tapon, L. Stowers, P.D. Burbelo, P. Aspenstrom, T. Bridges, J. Chant, and A. Hall. 1996. Rac and cdc42 induce actin polymerization and G1 cell cycle progression independently of $p65^{PAK}$ and the JNK/SAPK MAP kinase cascade. *Cell.* 87:519–529.

Lasa, I., E. Gouin, M. Goethals, K. Vancompernolle, V. David, J. Vandekerckhove, and P. Cossart. 1997. Identification of two regions in the N-terminal domain of ActA involved in the actin comet tail formation by *Listeria monocytogenes*. *EMBO (Eur. Mol. Biol. Organ.) J.* 16:1531–1540.

LaVallee, T.M., I.A. Prudovsky, G.A. McMahon, X. Hu, and T. Maciag. 1998. Activation of the MAP kinase pathway by FGF-1 correlates with cell proliferation induction while activation of the src pathway correlates with migra-

tion. *J. Cell Biol.* 141:1647–1658.
Lechler, T., A. Shevchenko, and R. Li. 2000. Direct involvement of yeast type I myosins in Cdc42-dependent actin polymerization. *J. Cell Biol.* 148:363–373.
Leng, J., R.L. Klemke, A.C. Reddy, and D.A. Cheresh. 1999. Potentiation of cell migration by adhesion-dependent cooperative signals from the GTPase Rac and Raf kinase. *J. Biol. Chem*. 274:37855–37861.
Liu, J., C. Huang, and X. Zhan. 1999. Src is required for cell migration and shape changes induced by fibroblast growth factor 1. *Oncogene*. 18:6700–6706.
Maa, M.-C., L.K. Wilson, J.S. Moyers, R.R. Vines, J.T. Parsons, and S.J. Parsons. 1992. Identification and characterization of a cytoskeleton-associated, epidermal growth factor sensitive pp60$^{c\text{-}src}$ substrate. *Oncogene.* 7:2429–2438.
Machesky, L.M., and A. Hall. 1997. Role of actin polymerization and adhesion to extracellular matrix in Rac- and Rho-induced cytoskeletal reorganization. *J. Cell Biol.* 138:913–926.
Machesky, L.M., and K.L. Gould. 1999. The Arp2/3 complex: a multifunctional actin organizer. *Curr. Opin. Cell Biol.* 11:117–121.
Machesky, L.M., and R.H. Insall. 1998. Scar1 and the related Wiskott-Aldrich syndrome protein, WASP, regulate the actin cytoskeleton through the Arp2/3 complex. *Curr. Biol*. 8:1347–1356.
Machesky, L.M., E. Reeves, F. Wientjes, F.J. Mattheyse, A. Grogan, N.F. Totty, A.L. Burlingame, J.J. Hsuan, and A.W. Segal. 1997. Mammalian actin-related protein 2/3 complex localizes to regions of lamellipodial protrusion and is composed of evolutionarily conserved proteins. *Biochem. J*. 328: 105–112.
Machesky, L.M., R.D. Mullins, H.N. Higgs, D.A. Kaiser, L. Blanchoin, R.C. May, M.E. Hal, and T.D. Pollard. 1999. Scar, a WASp-related protein, activates nucleation of actin filaments by the Arp2/3 complex. *Proc. Natl. Acad. Sci. USA.* 96:3739–3744.
Mandal, A., S. Naaby-Hansen, M.J. Wolkowicz, K. Klotz, J. Shetty, J.D. Retief, S.A. Coonrod, M. Kinter, N. Sherman, F. Cesar, C.J. Flickinger, and J.C. Herr. 1999. FSP95, a testis-specific 95-kilodalton fibrous sheath antigen that undergoes tyrosine phosphorylation in capacitated human spermatozoa. *Biol. Reprod.* 61:1184–1197.
Miglarese, M.R., J. Hannion-Henderson, H. Wu, J.T. Parsons, and T.P. Bender. 1994. The protein tyrosine kinase substrate cortactin is differentially expressed in murine B lymphoid tumors. *Oncogene.* 9:1989–1997.
Miki, H., T. Sasaki, Y. Taki, and T. Takenawa. 1998a. Induction of filopodium formation by a WASP-related actin-depolymerizing protein N-WASP. *Nature.* 391:93–96.
Miki, H., S. Suetsugu, and T. Takenawa. 1998b. WAVE, a novel WASP-family protein involved in actin reorganization induced by Rac. *EMBO (Eur. Mol. Biol. Organ.) J.* 17:6932–6941.
Mishima, M., and E. Nishida. 1999. Coronin localizes to leading edges and is involved in cell spreading and lamellipodium extension in vertebrate cells. *J. Cell Sci*. 112:2833–2842.
Mitchison, T.J., and L.P. Cramer. 1996. Actin-based cell motility and cell locomotion. *Cell.* 84:371–379.
Mullins, R.D., J.A. Heuser, and T.D. Pollard. 1998. The interaction of Arp2/3 complex with actin: nucleation, high affinity pointed end capping, and formation of branching networks of filaments. *Proc. Natl. Acad. Sci. USA.* 95: 6181–6186.
Naisbitt, S., E. Kim, J.C. Tu, B. Xiao, C. Sala, J. Valtschanoff, R.J. Weinberg, P.F. Worley, and M. Sheng. 1999. Shank, a novel family of postsynaptic density proteins that binds to the NMDA receptor/PSD-95/GKAP complex and cortactin. *Neuron.* 23:569–582.
Nobes, C.D., and A. Hall. 1995. Rho, Rac, and Cdc42 GTPases regulate the assembly of multimolecular focal complexes associated with actin stress fibers, lamellipodia, and filopodia. *Cell.* 81:53–62.
Ohoka, Y., and Y. Takai. 1998. Isolation and characterization of cortactin isoforms and a novel cortactin-binding protein, CBP90. *Genes Cells.* 3:603–612.
Olson, M.F., N.G. Pasteris, J.L. Gorski, and A. Hall. 1996. Faciogenital dysplasia protein (FGD1) and Vav, two related proteins required for normal embryonic development, are upstream regulators of Rho GTPases. *Curr. Biol.* 6:1628–1633.
Patel, A.M., L.S. Incognito, G.L. Schechter, W.J. Wasilenko, and K.D. Somers. 1996. Amplification and expression of EMS-1 (cortactin) in head and neck squamous cell carcinoma cell lines. *Oncogene.* 12:31–35.
Patel, A.S., G.L. Schechter, W.J. Wasilenko, and K.D. Somers. 1998. Overexpression of EMS1/cortactin in NIH3T3 fibroblasts causes increased cell motility and invasion in vitro. *Oncogene.* 16:3227–3232.
Peng, H.B., H. Xie, and Z. Dai. 1997. Association of cortactin with developing neuromuscular specializations. *J. Neurocytol.* 26:637–650.
Ridley, A.J., H.F. Patterson, C.L. Johnston, D. Diekmann, and A. Hall. 1992. The small GTP-binding protein Rac regulates growth factor induced membrane ruffling. *Cell.* 70:401–410.
Rinnerthaler, G., B. Geiger, and J.V. Small. 1988. Contact formation during fibroblast locomotion: involvement of membrane ruffles and microtubules. *J. Cell Biol.* 106:747–760.
Rohatgi, R., L. Ma, H. Miki, M. Lopez, T. Kirchhausen, T. Takenawa, and M.W. Krischner. 1999. The interaction between N-WASP and the Arp2/3 complex links Cdc42-dependent signals to actin assembly. *Cell.* 97:221–231.
Schafer, D.A., M.D. Welch, L.M. Machesky, P.C. Bridgman, S.M. Meyer, and J.A. Cooper. 1998. Visualization and molecular analysis of actin assembly in living cells. *J. Cell Biol.* 143:1919–1930.
Schoenwaelder, S.M., and K. Burridge. 1999. Bidirectional signaling between the cytoskeleton and integrins. *Curr. Opin. Cell Biol.* 11:274–286.
Schuuring, E., E. Verhoeven, H. van Tinteren, J.L. Peterse, B. Nunnink, F.B. Thunnissen, P. Devilee, C.J. Cornelisse, M.J. van de Vijer, W.J. Mooi, et al. 1992. Amplification of genes within the chromosome 11q13 region is indicative of poor prognosis in patients with operable breast cancer. *Cancer Res.* 52:5229–5234.
Servant, G., O.D. Weiner, P. Herzmark, T. Balla, J.W. Sedat, and H.R. Bourne. 2000. Polarization of chemoattractant receptor signaling during neutrophil chemotaxis. *Science.* 287:1037–1040.
Sheffield, P., S. Garrard, and Z. Derewenda. 1999. Overcoming expression and purification problems of RhoGDI using a family of "parallel" expression vectors. *Protein Expr. Purif.* 15:34–39.
Sheth, B., I. Fesenko, J.E. Collins, B. Moran, A.E. Wild, J.M. Anderson, and T.P. Fleming. 1997. Tight junction assembly during mouse blastocyst formation is regulated by late expression of ZO-1 alpha+ isoform. *Development.* 124:2027–2037.
Small, J.V., K. Rottner, and I. Kaverina. 1999. Functional design in the actin cytoskeleton. *Curr. Opin. Cell Biol.* 11:54–60.
Stevenson, B.R., J.D. Siliciano, M.S. Mooseker, and D.A. Goodenough. 1986. Identification of ZO-1: a high molecular weight polypeptide associated with the tight junction (zonula occludens) in a variety of epithelia. *J. Cell Biol*. 103:755–766.
Svitkina, T.M., and G.G. Borisy. 1999. Arp2/3 complex and actin depolymerizing factor/cofilin in dendritic organization and treadmilling of actin filament array in lamellipodia. *J. Cell Biol.* 145:1009–1026.
Tu, J.C., B. Xiao, S. Naisbitt, J.P. Yuan, R.S. Petralia, P. Brakeman, A. Doan, V.K. Aakalu, A.A. Lanahan, M. Shang, and P.F. Worley. 1999. Coupling of mGluR/Homer and PSD-95 complexes by the Shank family of postsynaptic density proteins. *Neuron.* 23:583–592.
Vuori, K., and E. Ruoslahti. 1995. Tyrosine phosphorylation of p130^{CAS} and cortactin accompanies integrin-mediated cell adhesion to extracellular matrix. *J. Biol. Chem.* 270:22259–22262.
Weed, S.A., Y. Du, and J.T. Parsons. 1998. Translocation of cortactin to the cell periphery is mediated by the small GTPase Rac1. *J. Cell Sci.* 111:2433–2444.
Weiner, O.D., G. Servant, M.D. Welch, T.J. Mitchison, J.W. Sedat, and H.R. Bourne. 1999. Spatial control of actin polymerization during neutrophil chemotaxis. *Nat. Cell Biol.* 1:75–81.
Welch, M.D., A.H. DePace, S. Verma, A. Iwamatsu, and T. Mitchison. 1997a. The human Arp2/3 complex is composed of evolutionarily conserved subunits and is localized to cellular regions of dynamic actin filament assembly. *J. Cell Biol.* 138:375–384.
Welch, M.D., A. Iwamatsu, and T. Mitchison. 1997b. Actin polymerization is induced by Arp2/3 protein complex at the surface of *Listeria monocytogenes*. *Nature*. 385:265–269.
Welch, M.D., J. Rosenblatt, J. Skoble, D.A. Portnoy, and T.J. Mitchison. 1998. Interaction of human Arp2/3 complex and the *Listeria monocytogenes* ActA protein in actin filament nucleation. *Science.* 281:105–108.
Wells, A., K. Gupta, P. Chang, S. Swindle, A. Glading, and H. Shiraha. 1998. Epidermal growth factor receptor-mediated motility in fibroblasts. *Microsc. Res. Tech.* 43:395–411.
Wiedmann, M., J.L. Bruce, C. Keating, A.E. Johnson, P.L. McDonough, and C.A. Batt. 1997. Ribotypes and virulence gene polymorphisms suggest three distinct *Listeria monocytogenes* lineages with differences in pathogenic potential. *Infect. Immun.* 65:2707–2716.
Wu, H., and K.T. Montone. 1998. Cortactin localization in actin-containing adult and fetal tissues. *J. Histochem. Cytochem.* 46:1189–1191.
Wu, H., and J.T. Parsons. 1993. Cortactin, an 80/85-kilodalton pp60^{src} substrate, is a filamentous actin-binding protein enriched in the cell cortex. *J. Cell Biol.* 120:1417–1426.
Wu, H., A.B. Reynolds, S.B. Kanner, R.R. Vines, and J.T. Parsons. 1991. Identification and characterization of a novel cytoskeleton-associated pp60^{src} substrate. *Mol. Cell. Biol.* 11:5113–5124.
Yates, J.R., III. 1998. Database searching using mass spectrometry data. *Electrophoresis.* 19:893–900.
Zhan, X., X. Hu, B. Hampton, W.H. Burgess, R. Friesel, and T. Maciag. 1993. Murine cortactin is phosphorylated in response to fibroblast growth factor-1 on tyrosine residues late in the G1 phase of the BALB/c 3T3 cell cycle. *J. Biol. Chem.* 268:24427–24431.
Zigmond, S.H. 1996. Signal transduction and actin filament organization. *Curr. Opin. Cell Biol.* 8:66–73.
Zitzer, H., D. Richter, and H.-J. Kreienkamp. 1999. Agonist-dependent interaction of the rat somatostatin receptor subtype 2 with cortactin-binding protein 1. *J. Biol. Chem.* 274:18153–18156.